Investigation of CO Deactivation of Passive NO<inf>x</inf> Adsorption on La Promoted Pd/BEA

Emission Control Science and Technology
https://doi.org/10.1007/s40825-021-00205-2

Investigation of CO Deactivation of Passive NO_x Adsorption on La Promoted Pd/BEA

Rojin Feizie Ilmasani[1] · Phuoc Hoang Ho[1] · Aiyong Wang[1] · Dawei Yao[1] · Derek Creaser[1] · Louise Olsson[1]

Received: 3 May 2021 / Revised: 29 October 2021 / Accepted: 8 November 2021

Abstract
Passive NO_x adsorption (PNA) is a method, in which NO_x can be stored at low temperatures and released at higher temperatures where the urea decomposition is functional during selective catalytic reduction (i.e., above 180–200 °C). We have studied the promotion of Pd/BEA with La as a PNA in the presence of high CO concentration. Both the reference and promoted samples exhibited a significant loss of NO_x adsorption/desorption capacity after multiple cycles using 4000 ppm CO. However, already after 5 cycles, 99% of the NO_x released between 200 and 400 °C was lost for Pd/BEA, compared to only 64% for Pd-La/BEA, which thereafter was stable. XPS and O_2-TPD clearly showed that the Pd species were influenced by La. The PNA deactivation in the presence of CO could be related to Pd reduction followed by migration and the formation of more PdO_x clusters, as observed by O_2-TPD analysis. Interestingly, significantly more PdO_x clusters formed on Pd/BEA after 10 cycles compared to Pd-La/BEA.

Keywords Cold start · PNA · Palladium zeolite · Lanthanum · Catalyst deactivation

1 Introduction

Lean-burn engines have lower fuel consumption and improved fuel efficiency. Yet, there are some challenges involved by using this technology for exhaust after-treatment systems concerning the process of lean NO_x reduction. Selective catalytic reduction (SCR) and lean NO_x traps (LNT) have been the most efficient techniques for NO_x reduction for both lean-burn and diesel engines [1–4]. Both methods have limitations in deNO_x performance at low temperatures (below 200 °C). In SCR technology, temperatures higher than 180–200 °C are needed to decompose urea and generate gaseous NH_3; meanwhile, both methods (NH_3-SCR and LNT) have kinetic limitations at low temperatures that causes low efficiency [5–8]. Even fast SCR reactions have low conversion at temperatures lower than 175 °C [9], and in addition the NO_2 formation over the DOC is limited at low temperature. One possible solution for these limitations is to introduce an adsorbent to store NO_x at low temperatures and gradually release NO_x at higher temperatures (> 200 °C) where the SCR catalyst is efficient to produce N_2 and H_2O. This newly developed technology has been called passive NO_x adsorption (PNA) [8]. Supported noble metals such as Pt, Pd, and Ag have been mostly studied as adsorbers for this method [6, 10–12]. Crocker et al. used Pt and Pd supported on CeO_2-ZrO_2 as an adsorber for PNA processes and the addition of Pt and Pd significantly increased NO_x adsorption performance [13]. In other studies, Ag/Al_2O_3 and Pt/Al_2O_3 were found to be capable of storing NO_x at temperatures lower than 200 °C [10, 14], but for Ag/Al_2O_3 the introduction of a small amount of H_2 was needed [14]. However, later it was found that these materials can undergo severe deactivation during NO_x adsorption due to sulfur poisoning from SO_2 which is inevitably present in exhaust emissions [15, 16].

Therefore, new attempts have focused on Pd supported on zeolites such as BEA, CHA, and MFI, where Chen et al. showed significant stability of Pd zeolite for PNA during sulfidation [15]. Moreover, Zheng et al. provided an increased understanding on atomic level of Pd dispersion and NO_x adsorption sites among different Pd-supported zeolites [17]. Regarding the Pd species, they reported that the active sites for NO adsorption are Pd^{2+} and Pd^{4+} which are in the form of PdO and PdO_2 respectively. They also

✉ Louise Olsson
louise.olsson@chalmers.se

[1] Chemical Engineering, Competence Center for Catalysis, Chalmers University of Technology, Se-412 96, Göteborg, Sweden

Published online: 25 November 2021

claimed that in wet NO TPD, the main adsorption sites are Pd^{2+} species [17].

In addition, a few studies have focused on adding promoters to the PNA material. Crocker et al. were one of the first groups that studied different promoters of Pt/Pd on Al_2O_3 and CeO_2. Regarding lanthanum as a promoter, which is of interest for this study, they observed a beneficial behavior on the PNA process for Pt/Al_2O_3, Pt/CeO_2, and Pd/CeO_2 [6]. Ji et al. also found that La as a promoter for Pt/Al_2O_3 resulted in an increase in the NO_x adsorption efficiency below 250 °C [10]. In our previous study, we concluded that La promotion of Pd/BEA had a positive effect by shifting the NO_x desorption to temperatures higher than 200 °C which is favorable for PNA performance [18].

Regarding the effect of CO on the adsorption and desorption of NO_x, Vu et al. examined the effect of CO addition on NO_x storage/desorption on Pd/BEA and it was found that the presence of CO causes more NO_x adsorption at lower temperatures and it also increases the desorption temperature window to higher values [19]. However, in the recent study by Yuntao et al., it was shown that repeated NO_x storage and release cycles with CO caused a gradual deactivation of the Pd/zeolites for NO_x adsorption [20]. This was also studied by Theis et al. using BEA, CHA, and ZSM5 zeolites with Pd and Pt, where it was observed that the performance degraded during repeated NO_x adsorption tests in the presence of high CO levels [21].

Therefore, improved adsorbent stability is critical for the application. Considering the beneficial effect of La promotion on the NO_x adsorption window as we reported previously, we investigate in the current study the stability of La-promoted Pd/BEA during sequential NO TPD experiments in the presence of high concentrations of CO. According to our knowledge, this is the first study where the stability of La-promoted Pd/zeolites are examined. The PNA materials were thoroughly characterized using ICP-SFMS, BET, O_2-TPD, STEM, XRD, XPS, and in-situ DRIFT spectroscopy, in order to gain a better understanding of the degrading effects of CO on adsorbent properties with and without La promotion.

2 Experimental Methods

2.1 Catalyst Preparation

The catalysts in this study were prepared using incipient wetness impregnation and were calcined at 500 °C for 5 h in air. Pd/BEA is used as the reference PNA, containing 1 wt.% Pd on Beta zeolite with a SAR (SiO_2-to-Al_2O_3 molar ratio) of 38 (CP814C, from Zeolyst International). A solution of Pd $(NO_3)_2$ (Sigma-Aldrich) and MilliQ water (Millipore) with a total volume equivalent to the pore volume of the support material was added dropwise to the support material. After the addition of the corresponding amount of Pd, it was dried overnight at 100 °C and thereafter calcined.

The lanthanum (La) containing PNA were synthesized with a La loading of 2.7 wt.%. According to our previous study [18], the 2.7 wt.% Lanthanum loading had the desired desorption window between 200 and 400 °C [21]. Accordingly, the used precursor material was lanthanum (III) nitrate hydrate (Sigma-Aldrich) which was added by two different sequential loading methods. One sample was prepared by first adding lanthanum followed by Pd and for the second sample, the promoter was loaded onto a portion of the batch of reference sample which had undergone Pd loading first. Both samples were dried overnight at 100 °C between the steps and calcined for 5 h at 500 °C after loading of each material. The samples are denoted corresponding to their loading sequence on the zeolite support (e.g., in La-Pd/BEA, La was loaded first). One Pd free sample was prepared with the same method, containing only 2.7 wt.% lanthanum loading on the zeolite support.

A washcoated monolith was prepared for each sample and was used for further activity measurements in the flow reactor. Cordierite monoliths (cpsi of 400), with 2 cm in length and 2.1 cm in diameter were used and they were prior to coating put in an oven for 2 h in air at 550 °C. The monoliths were washcoated using a slurry composed of approximately 90 wt.% liquid phase (equal amounts of water and ethanol) and 10 wt.% solid phase. The solid phase contained the PNA (95%) and binder (5% boehmite, Dispersal P2). Ethanol has been used in many studies for washcoating monoliths with Pd containing materials; therefore, for better comparison in this paper, the same ratio was used for this purpose. It should be noted that all the used samples had undergone a degreening step at 750 °C with 400 ppm NO, 8% O_2, and 5% H_2O. According to Lardionois et al. [22], high temperature treatment in air (i.e., high O_2 concentrations) results in more uniform Pd distributions. Each monolith was coated stepwise and between each step dried with a heating gun at around 90 °C for 2 min. This procedure was repeated until the total weight of washcoat was ~ 700 mg. Finally, the monoliths were calcined for 2 min at 500 °C with a heating gun and then calcined in an oven at 500 °C for 5 h (ramping with 2 °C/min).

2.2 Characterization

For determination of the BET surface area of the calcined samples, N_2 physisorption was done with a Tristar 3000 (Micromeritics) instrument. The samples were degassed in N_2 at 220 °C overnight. Elemental analysis (for Pd, La) was done by ICP-SFMS by ALS Scandinavia AB.

Transmission electron microscopy analysis was performed for reacted (scraped from monoliths) and degreened

powders. This was done using a FEI Titan 80-300 TEM. The degreened powder samples had undergone the degreening treatment (at 750 °C with 400 ppm NO, 8% O_2, 5% H_2O, and Ar) in a crucible in the flow reactor. Whereas, reacted samples were scraped from the monolith after 10 TPD cycles in the flow reactor, see Section 2.3. The powder samples were pestled in an agate mortar and added on copper TEM grids. The average particle size was calculated by ImageJ software using > 250 particles with diameter measurement from the particle areas.

Oxygen TPD experiments were carried out with a powder flow reactor equipped with mass flow controllers for gas feed and a Hiden HPR-20 QUI mass spectrometer. Approximately, 50 mg powder samples (both degreened and reacted samples) were loaded in the quartz tube. The measurements started with 3 vol% oxygen/Ar at a flow of 20 ml/min at 25 °C for 5 min, followed by heating up to 400 °C under the same gas conditions for 30 min. The experiment was followed by cooling down to room temperature with the same gas mixture and maintaining the same condition for 30 min. After 1 h of Ar flushing at room temperature, the desorption step was started by increasing the temperature to 800 °C at a rate of 20 °C/min in the presence of Ar only.

X-ray photoelectron spectroscopy (XPS) analysis was conducted using a PHI5000 VersaProbe III system equipped with a monochromatic Al K X-ray source (E = 1486.6 eV). C1s with the binding energy of 284.8 eV was used as a reference. The used samples consisted of degreened and reacted PNA. PdO material from Sigma-Aldrich (99.97%) was used as a reference for comparison. Power X-ray diffraction (XRD) was performed in a SIEMENS diffractometer D5000 which operates with Cu Kα radiation (λ = 1.5418 Å) at 40 kV and 40 mA. The data collection range was between 5° and 60° using a step size of 0.04.

2.3 NO TPD Measurement in the Flow Reactor

NO adsorption/desorption measurements were performed to investigate the CO effect on different adsorbents using a flow reactor setup. See reference [18] for a detailed description. In the quartz tube reactor, the monoliths were placed, and the tube was surrounded by a heating coil and insulating material. For temperature measurements, two type-K thermocouples were used, where one was placed in the monolith and one 15 mm before the sample. The outlet gas composition was measured with an MKS Multi-Gas 2030 HS FTIR. All experiments were performed with Ar as a balance and at atmospheric pressure. The total flow during TPDs was 900 Nml min^{-1} and during degreening 3500 Nml min^{-1}.

The degreening step was conducted to obtain a better distribution of Pd particles and formation of more ion-exchanged Pd species in the adsorbents [23]. This step is known to be sufficient either with a long period of high temperature (~ 750 °C) exposure to oxygen and water or by having a relatively high concentration of NO at high temperature in shorter durations [23, 24]. Therefore, the degreening step used in this study consisted of 1 h at 750 °C with 400 ppm NO, 8% O_2, 5% H_2O with an Ar balance, and then the samples underwent 10 TPD cycles. First, the PNA was exposed to 200 ppm NO, 4000 ppm CO, 8% O_2, 5% H_2O in Ar at 80 °C for 1 h. Thereafter, temperature ramping up to 500 °C at a rate of 20 °C/min was conducted, using the same gas mixture. Prior to each NO_x adsorption and TPD cycle, a pretreatment was performed at 500 °C with 8% O_2, 5% H_2O in Ar for 15 min. All the cycles were carried out using the same gas composition and same time intervals.

An example of a blank-test (empty tube with no monolith) experiment is shown in Fig. S1 (Supplementary material). This experiment was conducted using 200 ppm NO, 200 ppm CO, 8% O_2, and 5% H_2O with a total flow of 1000 ml/min. Initially when the NO MFC opens, an overshoot of NO_2 was observed, which decreased to 2.5 ppm after some seconds. This small overshoot can be due to minor oxidation of NO in the gas supply tubing when running experiments with high O_2 concentration in the carrier gas. The results show that there was a small amount of NO_2 present in the gas phase.

2.4 In-situ DRIFT Spectroscopy

To further characterize the surface species, diffuse reflectance infra-red Fourier transformed spectroscopy (DRIFT) was conducted on degreened samples. The PNA was placed on a porous grid in a reaction cell equipped with CaF_2 windows. The samples were pretreated at 550 °C for 15 min in 8% O_2 and 1% H_2O in Ar as carrier gas. The water concentration of 1% was used, due to limitations of the device used in preventing the condensation of water. Thereafter, the sample was cooled down to 80 °C and the background was acquired with the same gas mixture. The experiment was continued by collecting the spectra with the introduction of 200 ppm NO, 1% H_2O, and 8% O_2 first for 15 min, and then subsequently 200 ppm NO, 4000 ppm CO, 1% H_2O, and 8% O_2 in Ar for 15 min. The temperature was increased to 550 °C while keeping the same gas mixture and maintaining that temperature for 15 min to represent the desorption step. It should be noted that the temperature was 550 °C in the gas phase in the end of the desorption step. However, the catalyst powder reaches significantly lower temperature due to the design of the heater in the Harrick cell, resulting in that the temperature in the catalyst powder would be around 340 °C. This TPD cycle was repeated three times for the DRIFTS analysis and a pretreatment step (15 min at 550 °C in 8% O_2, 1% H_2O, and Ar as carrier gas) was applied before each cycle. Between each cycle, backgrounds were acquired at 80 °C, before the new spectra were collected.

3 Results and Discussion

3.1 Characterization

The contents of Pd and La were determined by ICP-SFMS and are displayed in Table 1. For all samples, the Pd content was around 1 wt.% and the La loading was 2.7 wt.% for samples containing La. The BET surface area and pore volume for the support and all four samples are also given in Table 1. The surface area and pore volume were similar after the addition of 1% Pd, likely due to the low loading. After the addition of 2.7 wt.% La, a decrease in both pore volume and surface area was observed, which is due to blockage of the pores by the introduction of the quite high concentration of La.

The morphology of Pd particles in the two La samples was investigated by STEM analysis (Fig. 1). Calcined catalyst powder samples were degreened at 750 °C for 1 h in the presence of 500 ppm NO, 8% O_2, and 5% H_2O in Ar, before the STEM analysis. Note that ion-exchanged Pd atoms are very small and difficult to detect with STEM. According to the literature [10] and our previous work [18], it can be expected that the Pd dispersion in the presence of La can decrease. Ji et al. found that when adding 1 wt.% lanthanum to Pt/Al_2O_3, the Pt dispersion significantly decreased, and it was proposed to occur due to occupancy of the Al_2O_3 defect sites by La [10]. Hoost et al. reported that in the case of close contact of La with Pd, highly dispersed oxygen-rich Pd particles will diminish [25]. In our current study, the collected images revealed multiple agglomerated particles in the La-Pd/BEA sample and these agglomerations were mainly between 30 and 50 nm, whereas in the Pd-La/BEA sample the particles were mostly between 10 and 20 nm. According to EDX mapping, it can be concluded that the detected particles are associated with Pd and that La is fairly well dispersed (Fig. 2). In our earlier study, higher La loading was examined and for that case more La was in close contact with Pd particles [18]. The results indicate that by loading of Pd prior to La, one can achieve a better distribution of Pd particles.

The Pd-La/BEA exhibited larger NO storage, which will be discussed in Section 3.2 and this sample was therefore used for further characterization and compared to the reference sample (Pd/BEA). STEM images of degreened powder samples and reacted samples (scrapped off from the monoliths after the sample had undergone 10 cycles of NO_x TPD with the addition of 4000 ppm CO, see Section 3.2) are shown in Fig. 3. According to the measurements, it was observed that the average particle size for the two degreened samples was around 30 nm. However, the fluctuation of the average size is much higher in Pd-La/BEA (~ 18.2 nm). It should be noted that the STEM cannot detect the ion-exchanged Pd and that DRIFTS results (see Section 3.3) indicate a large amount of ionic Pd species. Thus, the STEM results only reveal information about the Pd particles, which provide less NO storage [26].

Table 1 Pd and La loadings (measured by ICP-SFMS) and specific BET surface area for each sample

Sample type	SiO_2/Al_2O_3 (SAR no.)	Pd content (wt.%)	La content (wt.%)	SBET (m^2/g)	Pore volume (cm^3/g)
BEA	38	–	–	636.2	0.35
Pd/BEA	37.7	1.1	–	630.6	0.36
La/BEA	36.5	–	2.7	516.1	0.30
La-Pd/BEA	36.5	0.9	2.7	555.1	0.32
Pd-La/BEA	37.1	1.1	2.7	540.0	0.32

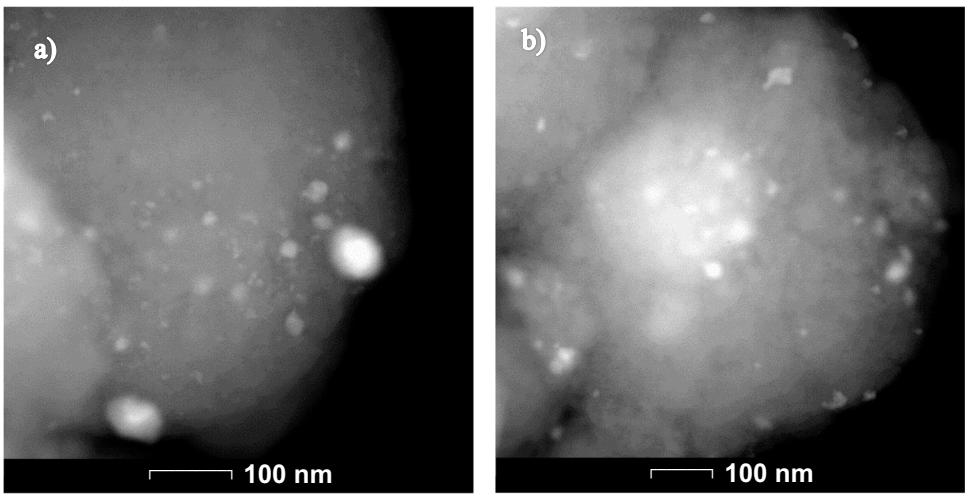

Fig. 1 STEM images for **a** La-Pd/BEA and **b** Pd-La/BEA at 100 nm magnification

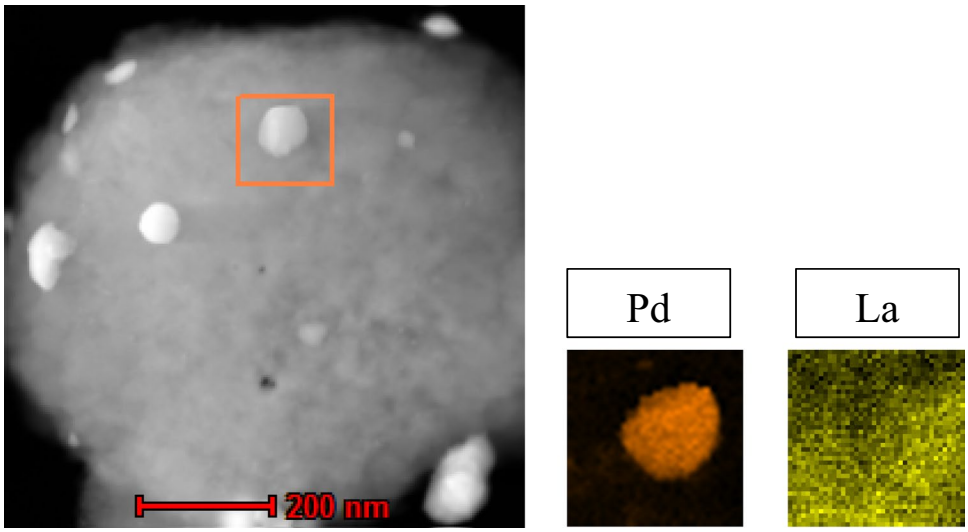

Fig. 2 EDX mapping images for La-Pd/BEA

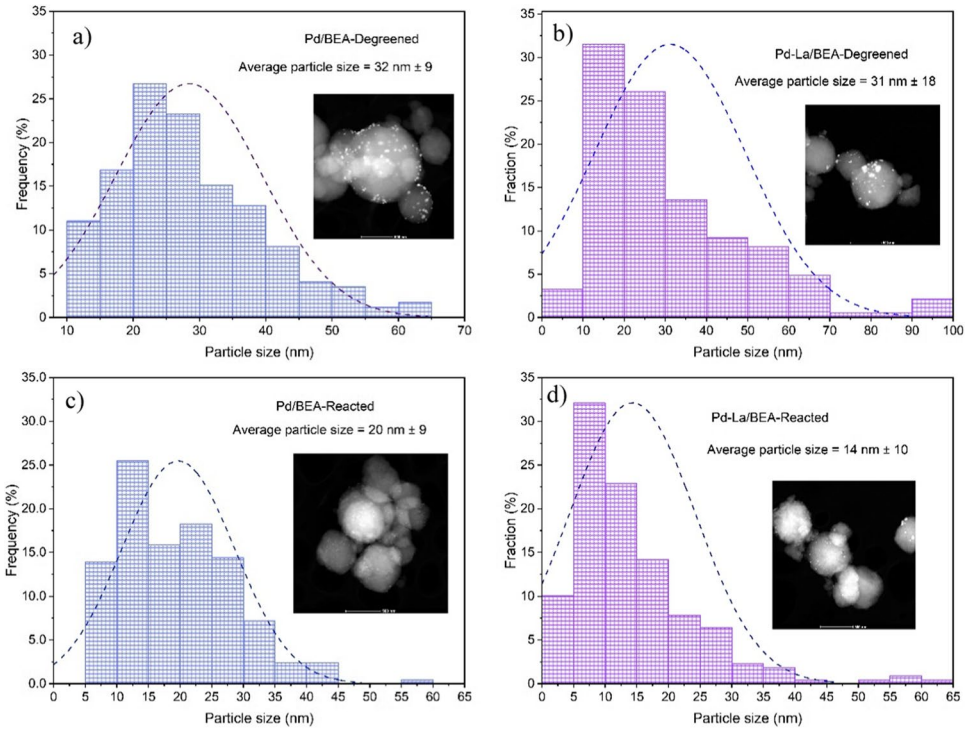

Fig. 3 STEM images and particle size fraction for degreened **a** Pd/BEA, **b** Pd-La/BEA and reacted **c** Pd/BEA, **d** Pd-La/BEA

The TEM analysis from the reacted samples (Fig. 3c, d) indicates that after 10 cycles, surprisingly the average particle sizes have decreased for both Pd/BEA (from 32 to 20 nm) and Pd-La/BEA (from 31 to 14 nm) samples. Yuntao et al. reported the formation of agglomerated Pd particles due to CO exposure in a Pd/BEA adsorbent which caused activity degradation [20]. We suggest that during CO aging, some of the ion-exchanged Pd (not detected in STEM) forms smaller Pd particles and that this is the reason for the decreased overall Pd particle size, i.e., in the reacted samples the Pd particles are a combination of the larger Pd particles from synthesis and smaller Pd particles formed during aging. In addition, a larger number of particles were found for the reacted Pd/BEA compared with reacted Pd-La/BEA, suggesting a larger formation of Pd particles during aging for Pd/BEA. These results agree with the O_2-TPD analysis, which will be discussed in the next paragraph.

The oxygen storage properties of the two samples (Pd/BEA and Pd-La/BEA) were studied with oxygen TPD. Both degreened and reacted samples (after 10 cycles of NO TPD in the presence of high CO levels) were used for O_2-TPD. In the degreened samples (Fig. 4a), two temperature ranges

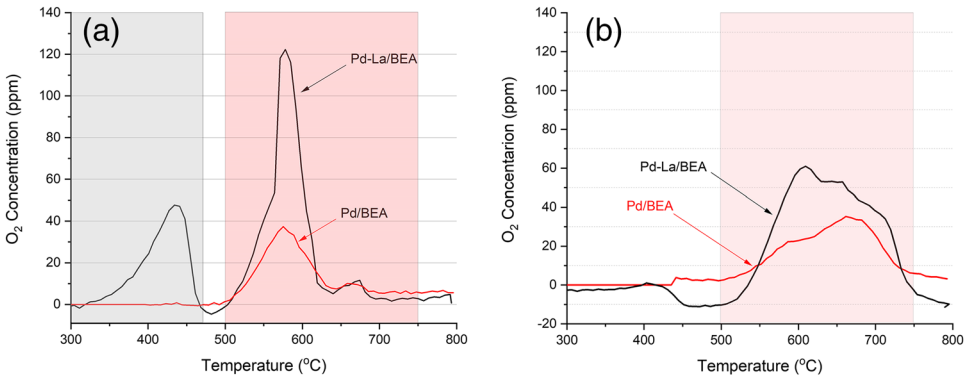

Fig. 4 O_2-TPD profile of **a** degreened Pd/BEA and Pd-La/BEA and **b** reacted Pd/BEA and Pd-La/BEA

for oxygen desorption can be observed. The first one is located between 300 and 475 °C for the degreened La promoted sample (maximum at 434 °C), which is assigned to desorption of surface adsorbed oxygen from PdO_x species [27, 28]. This peak corresponds to 31% of all released oxygen from this sample. However, since this peak is absent in the Pd/BEA sample, it could possibly be related to La_2O_3 present on the surface. Another O_2-TPD experiment was therefore conducted for the La/BEA sample (see Fig. S2 in Supplementary material) which showed that there is no O_2 desorption from La/BEA. This result indicates that the O_2 release is not from La_2O_3, but from the palladium. However, it cannot be ruled out that the Pd enhanced the desorption of oxygen from the lanthanum oxide. Hoost et al. detected a low-temperature oxygen peak in Pd/La-Al_2O_3, and they assigned it to oxygen produced from the oxidation of LaO_x forming species on the Pd particles [25]. The second desorption peak appeared between 500 and 650 °C and according to the literature, this is due to the release of O_2 from the decomposition of PdO_x clusters while ramping up to higher temperatures [28, 29]. Comparison of the reference sample and lanthanum modified sample in Fig. 4a indicates that the amount of oxygen release is higher for Pd-La/BEA compared with Pd/BEA. According to Hoost et al., this is due to the formation of new Pd-La_2O_3 sites by the interaction of highly dispersed palladium with the promoter in the form of mixed metal oxide [25].

For both adsorbents, we observed that the desorption peaks in the reacted samples are broadened with desorption at a higher temperature compared to the degreened sample, in the range of 500–750 °C. In the La-containing sample, the low-temperature peak at 434 °C was drastically reduced after the reaction. This can be explained by the reduction of Pd species after CO exposure, which led to a loss of Pd/La sites that adsorbed more loosely bound oxygen.

Integration of the released oxygen showed that the amount of desorbed oxygen is 1.1 times higher for the reacted Pd-La/BEA sample compared to its corresponding degreened state. On the other hand, for Pd/BEA, the reacted sample exhibited 1.7 times higher oxygen desorption than the degreened sample. The same O_2-TPD process was performed on the La/BEA (Pd free) sample and no adsorption nor desorption of oxygen was detected for the degreened or reacted sample (Fig. S2). This is due to the high stability of La oxide at high temperatures [30], and it can be concluded that the oxygen uptake of the Pd-La/BEA sample is related to Pd metal and Pd sites in close interaction with La.

As described earlier, the high-temperature desorption of oxygen can be assigned to the decomposition of PdO_x clusters [28, 29]. Since the high-temperature peak is significantly increased for the reacted Pd/BEA sample, it suggests that there is a large formation of PdO_x clusters during repeated cycling in the presence of high CO concentration, which is in accordance with the STEM analysis (Fig. 3). Interestingly, the increase in O_2 release is much smaller for Pd-La/BEA, which suggests that the sample is more stable toward PdO_x formation. For dry PNA processes, adsorption of NO_x is occurring on both ionic Pd (Pd^{2+}) and PdO_x (Pd^{4+}) species [17]. However, Zheng et al. reported that under wet conditions, ionic Pd is the main species for NO adsorption [17]. Moreover, several studies reported that when exposing the PNA to high CO concentrations, Pd^{2+} forms Pd particles [21, 31, 32]. Yuntao et al. also reported that the reduced Pd^{2+} species form Pd^0 which thereafter are converted to palladium particles [20]. Our oxygen TPD results clearly show an increase in PdO_x clusters/particles after reaction for the reference sample in this study, which we suggest is the main reason for the activity degradation. Since we perform a high-temperature oxygen pretreatment between each TPD experiment, it is likely that we oxidize the formed Pd particles to PdO_x particles. Interestingly, the Pd-La/BEA forms significantly less PdO_x particles during long-term CO exposure, as seen by the O_2-TPD experiments. When examining the desorption peaks for reacted samples (Fig. 4b), it can be seen that although the oxygen release started at 500 °C (same as degreened samples), the desorption peak broadened to 750 °C. It has been reported that at high temperatures, the decomposition of PdO_x species, has a direct relation with the oxidation state of Pd and oxygen coordination number [28]. Meaning that a broader desorption peak for reacted

samples can originate from more PdO_x species and higher oxygen coordination which can lead to higher desorption temperatures [28].

Figure 5 shows the XP Pd 3d spectra of Pd/BEA and Pd-La/BEA degreened and after CO exposure. As a reference, a commercial bulk PdO sample showed two peaks of Pd^{2+} located at 336.9 eV ($3d_{5/2}$) and 342.4 eV ($3d_{3/2}$) [5] (lower panel in Fig. 5). Comparing the degreened and reacted Pd/BEA, an obvious shift to lower binding energy (from 337.5 to 336.8 eV) after CO exposure is observed, which is due to the reduction of Pd species. As it was mentioned before, with a high concentration of CO, ionic Pd particles can be reduced, leading to more cluster formation which was confirmed with O_2-TPD (Fig. 4). Comparing the degreened samples of Pd/BEA and Pd-La/BEA, a shift toward lower binding energy is observed for Pd-La/BEA sample, i.e., Pd is in a lower valance state. This was also detected in our previous work when comparing Pd-5.4%La/BEA with Pd/BEA [18]. These results show that La is influencing the Pd, which was also seen during oxygen TPD where the degreened Pd-La/BEA sample exhibited a desorption peak at low temperature which was not the case for Pd/BEA (Fig. 4a).

For Pd/BEA on the other hand, the shift for this sample after CO exposure was toward higher binding energies, which is surprising. The reason could be Pd particle migration out to the surface, which is followed by oxidation of the Pd clusters during the oxygen treatment between each cycle. Overall, the oxidation states for both Pd/BEA and Pd-La/BEA after reaction are similar.

It is known that the XPS signal mostly detects the first few nm of the surface of particles [33]. Therefore, some quantifications were done based on the relative surface concentration of palladium [23]. Considering this, the integration of the Pd peaks showed that in the Pd/BEA sample the relative surface concentration of Pd was decreased about 16% after reaction, and this value was about 6% for the lanthanum modified sample. This indicates that more Pd particles formed clusters on the surface of the reference sample, thus less area was detected in XPS, which is in line with the O_2-TPD measurements (Fig. 4).

Figure 6 presents the XRD patterns of Pd/BEA and Pd-La/BEA revealing the crystallinity of the degreened and reacted powders. Since the reacted powder was scrapped off from the monoliths, there is a risk that some cordierite and also the binder is present in the XRD measurement. We therefore performed the same measurement for an uncoated degreened cordierite monolith and for the binder which has been used in the coating process (Fig. S3). This was done to ensure that the peaks were originating from the catalyst and to distinguish any possible overlaps.

Peaks at $2\theta = 21.5°$ and 22.5° in both of the samples are related to the morphology of BEA [20]. Two specific Pd peaks were observed at $2\theta = 33.8°$ and 40.2° and they are

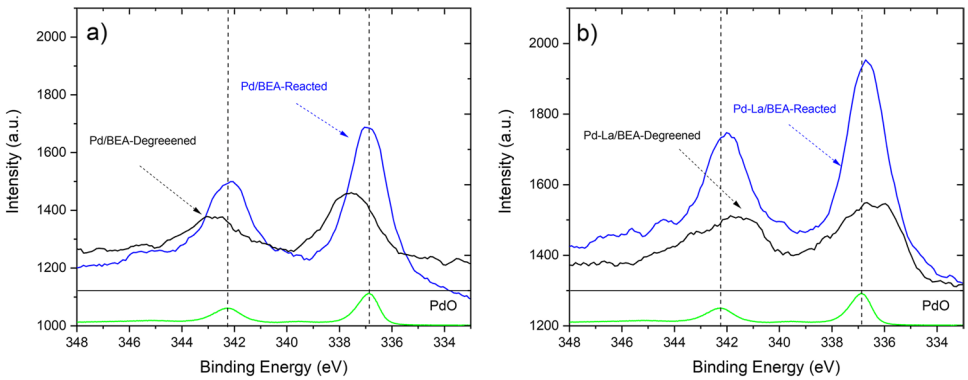

Fig. 5 Pd 3d XPS spectra for the **a** Pd/BEA and **b** Pd-La/BEA degreened and reacted, using PdO as a reference

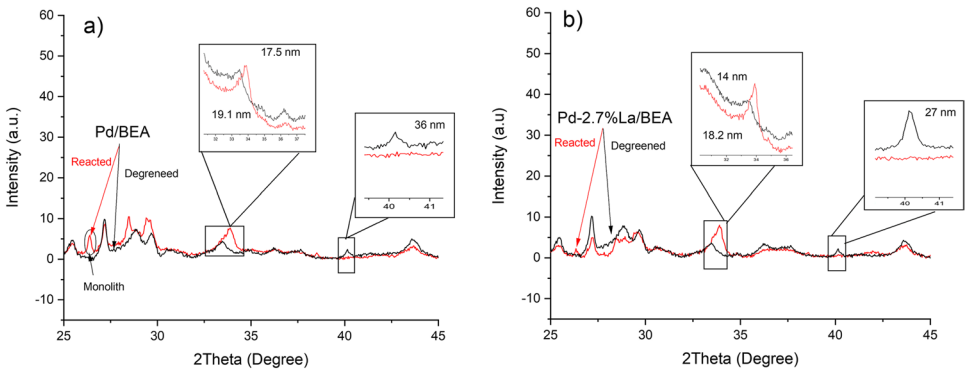

Fig. 6 XRD patterns of degreened and reacted **a** Pd/BEA and **b** Pd-La/BEA samples

assigned to PdO and Pd respectively [20, 34]. In both samples, the Pd peak at 2θ = 40.2° disappeared after the multiple CO exposure experiment, but the peaks at 2θ = 33.8° grew after the reaction. The formation of more PdO_x clusters/particles after repeated CO experiments is in line with the O_2-TPD experiments (Fig. 4). We propose that during the 10 TPD cycles, the Pd is reduced and formed small Pd particles which during the pretreatment between the cycles formed PdO_x particles. Figure 6 indicates a shift for the Pd related peak at 2θ = 33.8° after the reaction. This shift occurred due to the increased area of the peak and according to Bragg's equation ($d = {}^{n\lambda}/_{2sin\theta}$), which can be due to shrinkage of the palladium lattice planes after the CO exposure [35]. Comparing the La/BEA and Pd/BEA spectra (Fig. S4), it is clear that there is no additional peaks in La/BEA related to lanthanum. Kim et al. also did not observe any peaks related to lanthanum for 3 wt.% La in Pd-La/Al_2O_3 [36].

3.2 Temperature Program Desorption Experiments

Figure 7 shows the NO_x desorption profiles for the first cycle of the two La-containing adsorbents, where the La was added in different orders (Pd-La/BEA and La-Pd/BEA). Both samples underwent adsorption followed by temperature-programmed desorption with 200 ppm NO, 4000 ppm CO, 5% H_2O, and 8% O_2 in Ar at 80 °C, followed by a ramp to 500 °C, respectively. It was found that loading Pd prior to La increased the desorption quantity at high temperatures (above 200 °C) by 48%. This could be due to better Pd distribution in this sample which was supported by TEM analysis (Fig. 1). It is possible that when adding La first, it blocks the access to some of the Brönsted acid sites and thereby lowers the amount of ion-exchanged Pd. It was found that the addition of La clearly decreased both the BET surface area and pore volume (Table 1), which supports the hypothesis that access to Brönsted acid sites was reduced. The adsorption of NO in Pd-La/BEA occurred continuously until approximately 160 °C and then the desorption started at 170–190 °C, and subsequently continued and resulted in a second desorption peak from 250 to 500 °C. According to the literature, initially, NO_x can be adsorbed on weaker sites, and then gradually spillover to stronger adsorption sites [10]. Meaning that some of the sites that are kinetically inaccessible during the adsorption step can be accessible during ramping up. Based on these experiments, we can conclude that the order of the metal addition significantly influences the NO_x adsorption and desorption process. Due to the favorably higher NO_x desorption above 200 °C for the Pd-La/BEA sample, it was used for further experiments and characterization.

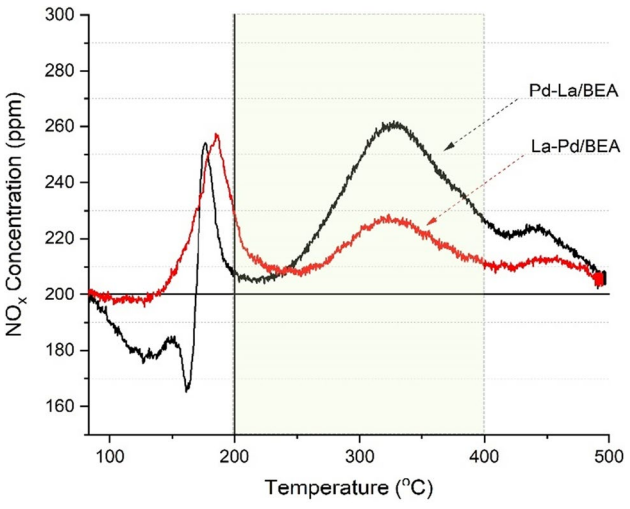

Fig. 7 NO_x concentration for first TPD experiment with 8%O_2, 5%H_2O, 200 ppm NO, and 4000 ppm CO for La-Pd/BEA and Pd-La/BEA samples

Multiple cold start events occur in a vehicle exhaust; therefore, it is important to examine how the adsorbent's behavior changes after several TPD experiments. Both Yuntao et al. [20] and Theis et al. [21] have found that CO addition for prolonged periods was detrimental for Pd/zeolites used as PNAs, and we have therefore included 4000 ppm CO in our repeated TPD experiments. Initially, all the samples were degreened for 1 h at 750 °C, cooled down to 80 °C, where the adsorber was exposed to 200 ppm NO, 4000 ppm CO, 8% O_2, 5% H_2O in Ar at 80 °C for 1 h followed by a temperature ramp in the same gas mixture. This TPD cycle was repeated 10 times with an oxygen-containing pretreatment in between (see Section 2.3). The results are presented in Fig. 8 for Pd/BEA and the Pd-La/BEA samples.

For Pd/BEA, a large desorption peak was observed around 170 °C and in addition a broad peak between 300 and 400 °C. The total NO storage gives a NO_x/Pd ratio of 0.33. This shows that besides ion-exchanged Pd, there are also Pd clusters and particles present, which is consistent with the TEM images (Figs. 2 and 3) and O_2-TPD (Fig. 4). As will be discussed in connection to the DRIFTS experiments for Pd/BEA (Section 3.3), a large amount of linear nitrosyl species were observed, where NO is adsorbed on the ion-exchanged Pd (Pd^{2+}-NO) [5, 24]. Moreover, the peak at 170 °C is mainly associated with NO desorption (see Fig. S5). We therefore suggest that the large desorption peak around 170 °C is related to NO desorption from Pd^{2+} sites ($Z^-Pd^{2+}(NO)Z^-$). In addition, some desorption could also be due to NO_x released from palladium nitrates, since also nitrates were observed in DRIFTS (Section 3.3). Zheng et al. reported that the two adsorption sites that are formed by Pd^{2+} in the wet condition [17] are as follows:

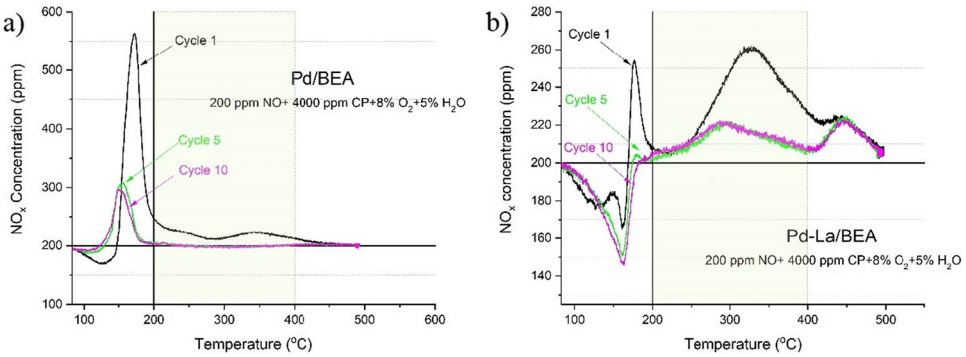

Fig. 8 NO_x concentration for repeated TPD experiments with 8% O_2, 5% H_2O, 200 ppm NO, and 4000 ppm CO for a) Pd /BEA and **b** Pd-La/BEA. It should be noted that the *y*-axis scales in **a** and **b** are different

$$Z^{-}Pd^{2+}Z^{-} + NO \rightarrow Z^{-}Pd^{2+}(NO)Z^{-} \quad (1)$$

$$3NO + 2Z^{-}[Pd(II)OH)]^{+} \rightarrow 2Z - Pd^{+}(NO) + NO_2 \quad (2)$$

Indeed, an NO_2 release peak was observed here at 244 °C, which could be due to reaction (2). It is therefore possible that the desorption of NO_x at higher temperature is related to desorption of NO from the 2Z-Pd^{+}(NO). It should be noted that at high temperature NO oxidation is active over the Pd sites, resulting in NO_2 formation.

It was found that for the Pd/BEA sample during the first five cycles, ~ 65% loss occurred for the NO_x release below 200 °C, but the deactivation slowed down and between the 5th and 10th cycle a further decrease by 11% in NO_x release was found. However, 99% of the NO_x desorbed at temperatures above 200 °C disappeared after five cycles for Pd/BEA. Theis and Ura also studied the behavior of multiple NO_x storage tests on a Pd/BEA catalyst with 900 ppm CO and 300 ppm H_2 and the results also showed a degradation in the performance caused by the addition of the reducing agent in the gas mixture, which was suggested to be due to CO induced Pd sintering [21]. The formation of Pd particles from sintering of ion-exchanged palladium is likely the reason also for our large drop in NO storage on Pd/BEA.

The corresponding cycling results for Pd-La/BEA are shown in Fig. 8b. The desorption peak around 170 °C for Pd-La/BEA is occurring at similar temperature as for the Pd/BEA sample and we therefore suggest that it is relating to NO desorption from Pd^{2+} sites. The broad desorption peak from 200 to 400 °C can be assigned to stronger bonds, such as 2Z-Pd^{+}(NO) which was suggested for Pd/BEA, but also NO species that are formed over the ion-exchanged Pd sites interacting with La and nitrates formed on La sites. The final desorption peak at temperatures higher than 400 °C is completely related to NO_2 and is likely originating from decomposition of nitrates on the lanthanum and lanthanum in close connection to Pd. The NO_x/Pd ratio for degreened sample was 0.24, which is lower than for Pd/BEA (0.33). These results suggest that there are more PdO_x species on the Pd-La/BEA sample, resulting in a lower overall storage for the degreened sample. This is in line with the O_2-TPD results for degreened samples (Fig. 4a), where larger O_2 desorption was observed for Pd-La/BEA sample. It is also possible that since La was added as a last step in catalyst synthesis that the La is blocking some pores, as can be seen by a decreased BET surface area (Table 1) and thereby hindering access to some Pd sites. This could be another reason for the lower NO_x/Pd ratio. However, the broad peak between 200 and 400 °C is 72% larger for Pd-La/BEA compared to Pd/BEA, which clearly shows that new storage sites are also present for Pd-La/BEA.

The results in Fig. 8b shows that the presence of La results in a more stable behavior of the desorption after the 5th cycle. In this sample, the degradation in NO_x desorption was about 64% for temperatures above 200 °C from the first to the 5th cycle and from the 5th to 10th cycle, there is no further loss in the amount of NO_x released. Moreover, it can also be seen that the desorption peak at temperatures less than 200 °C disappears and the NO_x storage around 160 °C increases for each cycle. These results indicate that the cycling experiments result in a gradual increase in the activation energy for NO storage, since the temperature for NO adsorption is increasing. The increased stability for the Pd-La/BEA compared to Pd/BEA could be due to less formation of PdO_x clusters for the promoted sample after exposure to CO, as suggested from the oxygen TPD experiments (Fig. 4b).

To further elucidate the role of lanthanum in NO adsorption/desorption in Pd-La/BEA, a La/BEA sample was studied with the same reactor conditions (Fig. 9). In this sample, one desorption peak around 350 °C was found for the degreened sample, which is at a higher temperature compared to the Pd-La/BEA sample (327 °C). Stable desorption behavior was achieved from the second cycle and the deactivation was remarkably smaller compared with the two Pd-containing samples (Fig. 8).

In order to facilitate a comparison between the samples, the NO_x desorption was integrated, and the results are shown in Table 2. The objective of the PNA is to store NO_x and

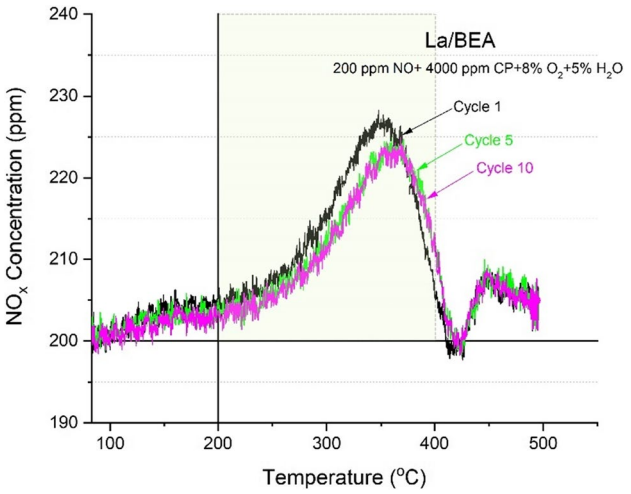

Fig. 9 NO_x concentration for repeated TPD experiments with 8% O_2, 5% H_2O, 200 ppm NO, and 4000 ppm CO for La/BEA

Table 2 Specification of NO_x desorption peaks in La/BEA, Pd/BEA, and Pd-La/BEA

	Cycles	P1 (<200 °C)		P2 (200 °C<x<400 °C)	
		NO_x (μmol)	Peak temp	NO_x (μmol)	Peak temp
La/BEA	1	0.31	–	5.59	351 °C
	5	0.34	–	4.87	363 °C
	10	0.37	–	4.70	364 °C
Pd/BEA	1	13.0	172 °C	8.30	345 °C
	5	4.6	156 °C	0.08	–
	10	4.1	152 °C	0.01	–
Pd-La/BEA	1	1.13	177 °C	14.3	327 °C
	5	0.03	–	5.20	296 °C
	10	0.06	–	5.71	289 °C

release it when the SCR catalyst is fully operating, which is above about 200 °C. In addition, the NO_x should not be released at too high temperature, since there is a risk that it will prevent proper regeneration. We have therefore examined the amount of NO_x release below 200 °C (denoted P1) and between 200 and 400 °C (denoted P2) and the values are shown in Table 2. The NO_x release is a combination of NO and NO_2, which can be seen in Figs. S5–S7, where the full experiments are shown. For the Pd/BEA sample, desorption at low temperatures is the main NO_x release in all the cycles. Examination of the NO and NO_2 concentrations (Fig. S5) indicates that desorption from Pd/BEA was mostly related to NO and the main peak was found at 172 °C. The sample possessed some NO oxidation activity likely related to PdO_x particles [37], with about 30% conversion at 500 °C. There is a NO_2 peak and simultaneously an NO consumption peak at about 470 °C. However, there is no clear NO_x release occurring at the same temperature. This NO_2 is therefore likely related to NO oxidation. NO oxidation is an equilibrium-limited reaction and therefore the NO_2 formation decreases at high temperature.

For Pd-La/BEA (Table 2), it is clear that the major release of NO_x is at higher temperatures, which is in line with our earlier study [18]. Comparing Pd/BEA and Pd-La/BEA (Table 2) indicates that the Pd-La/BEA sample released 42% more NO_x in the temperature interval 200–400 °C, compared to Pd/BEA. The Pd-La/BEA sample releases both NO as well as NO_2 (see Fig. S6). The NO_2 release can originate from adsorption of some amount of NO_2 in the inlet feed that can form nitrates, but also possibly due to nitrate formation from NO, since the sample has NO oxidation activity. Another source of NO_2 formation could be the transformation of $2Z^-[Pd(II)OH)]^+$ according to reaction 2 [17]. The La-BEA on the other hand stored and released less NO_x compared to Pd-La/BEA and the main release was between 200 and 400 °C. For La-BEA the NO_x release was due to NO_2 desorption and no NO desorption was involved (see Fig. S7). Thus, some of the NO_x released from Pd-La/BEA was likely originating from adsorbed NO_x on the La sites. The BEA zeolite contains extra-framework aluminum sites, which possibly could store NO_x. However, NO TPD experiments performed at 150 °C on pure BEA (same supplier BEA material) showed that the NO_x storage on pure BEA could be neglected [38]. Thus, the NO_x release for La/BEA observed between 200-400°C is associated with NO_x storage on the lanthanum.

The degreened Pd-La/BEA sample released 61% more NO_x below 400 °C, compared to La/BEA, thus both La and Pd sites were associated with the storage. The NO_x release occurred at a lower temperature for Pd-La/BEA (327 °C) compared to La/BEA (351 °C). These results suggest that the interaction between La and Pd facilitated the NO_x desorption. The characterization results clearly showed that the La addition affected the Pd species, where the La addition resulted in a lower oxidation state of Pd (Fig. 5) and less stable adsorbed oxygen on the Pd sites (Fig. 4). Moreover, the DRIFTS analysis indicated unique nitrate peaks formed on Pd-La/BEA compared with Pd/BEA and La/BEA (see Section 3.3).

Integrated NO_x release results for cycles 5 and 10 are also shown in Table 2. It is clear that the La/BEA sample is very stable, and the NO_x release only decreases between 200 and 400 °C by 16% in total (12% during the first 5 cycles). To conclude, the La stores some NO_x which is released in the form of NO_2, and it is quite stable also during 10 cycles with 4000 ppm CO. Pd/BEA on the other hand lost 68% of the NO_x storage at low temperature ($\lesssim$ 200 °C) during 10 cycles, of which 65% was lost during the first 5 cycles. For the NO_x release at medium temperature (200–400 °C), even more was lost, with a 99% loss

during the first 5 cycles and 99.8% in total for 10 cycles. Our results clearly show that Pd/BEA is largely deactivated by multiple cycles while being exposed to high CO concentrations which are in line with the studies by Yuntao et al. [20] and Theis et al. [21]. Interestingly, the NO_x released at medium temperature (200–400 °C) was more stable for the Pd-La/BEA sample compared with the Pd/BEA sample, where the Pd-La/BEA lost 64% from the first to the 5th cycles and from the 5th to 10th cycle there was no further loss in the amount of NO_x. Comparing the 10th cycle for La/BEA and Pd-La/BEA reveals that the Pd-La/BEA still released more NO_x (18%), but that the differences are significantly decreased. However, there are large differences in the transient behavior of the NO_x adsorption and release for the two samples, showing that the interaction between Pd and La is important. Firstly, the desorption of NO_x occurs in a more favorable temperature interval for Pd-La/BEA (289 °C), while it is in the upper-temperature region for La/BEA (364 °C). Secondly, the Pd-La/BEA is clearly adsorbing NO (see Figs. S6 and Fig. 8b) when increasing the temperature, which is not the case for La/BEA. Actually, for the Pd-La/BEA, 49% of the NO_x desorbed was adsorbed as NO during the temperature ramp for the 10th cycle.

3.3 In Situ DRIFTS Analysis

The different nature and quantities of adsorbed species was further investigated with in situ DRIFTS with the degreened samples. The samples were exposed to a 15-min pretreatment step at 550 °C followed by cooling to 80 °C. The PNA was exposed to 200 ppm NO, 1% H_2O, and 8% O_2 first for 15 min at 80 °C, and then 200 ppm NO, 4000 ppm CO, 1% H_2O, and 8% O_2 in Ar for an additional 15 min. Thereafter, the sample was heated up in the same gas mixture. The TPD cycle was repeated three times and the spectra were collected at the beginning of each of the 3 NO TPD cycles. Figures 10 and 11 compare the collected spectra for Pd/BEA and Pd-La/BEA during the adsorption at 80 °C, for the first step without CO and the following step with CO for each cycle.

The sharp peak in Fig. 10a at 1813 cm^{-1} is usually assigned to linear nitrosyl species where NO is attached to the cationic Pd^{2+} (Pd^{2+}-NO) which is located at the exchange sites [5, 23]. Peaks around 1633 cm^{-1} and 1653 cm^{-1} are assigned as NO_2 interacting with OH groups [10]. The second strongest peak at 1360 cm^{-1} can arise from the interaction of H_2O with HNO_2 [39]. The weak peak around 1567 cm^{-1} can be related to chelating bidentate nitrates [10]. At higher wavenumbers, two negative peaks around 2112 cm^{-1} and 2130 cm^{-1} are observed for the case without CO (Fig. 10a). Peaks at these positions can be assigned to linear CO on ionic Pd [19, 40] and Pd^{+}(CO)(OH) [41, 42].

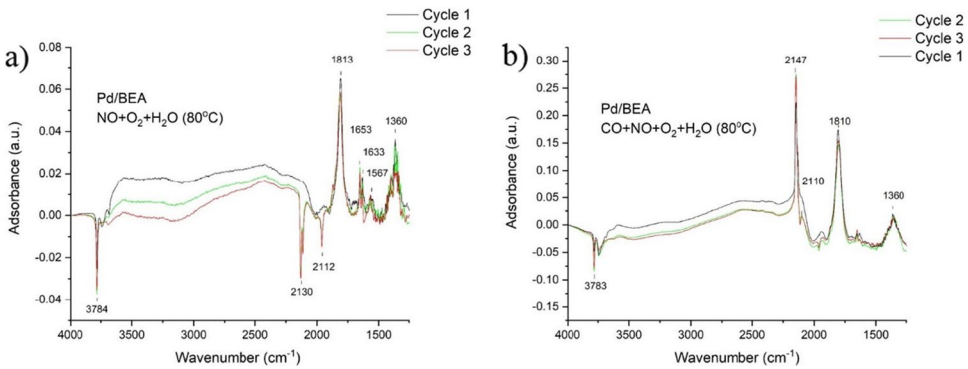

Fig. 10 DRIFT spectra for exposure of Pd/BEA to 8% O_2, 1%H_2O and 200 ppm NO at 80 °C **a** without CO and **b** with 4000 ppm CO

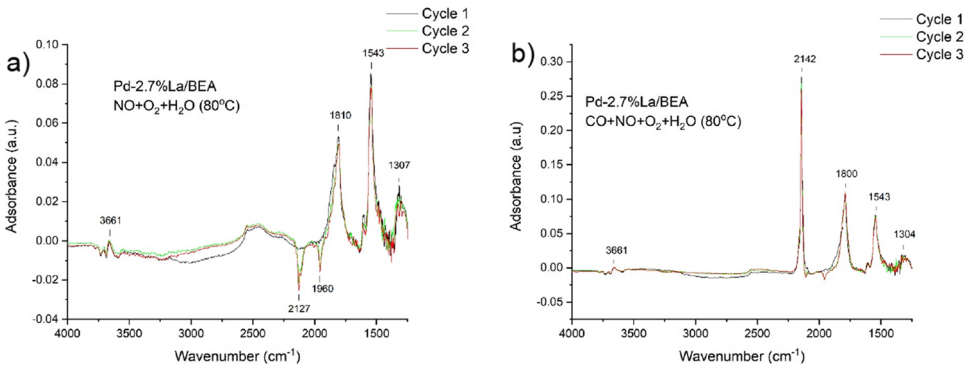

Fig. 11 DRIFT spectra for exposure of Pd-La/BEA to 8% O_2, 1%H_2O, and 200 ppm NO at 80 °C **a** without CO and **b** with 4000 ppm CO

These negative peaks are only seen for cycle 2 and 3, in the first adsorption part without CO (Fig. 10a). This suggests that NO can remove some of the linear CO on Pd^{+} and linear CO on ionic Pd during NO exposure without CO. The spectra shown in Fig. 10b for the case with the presence of 4000 ppm CO show that large positive bands are visible around 2110 cm^{-1} and 2147 cm^{-1}, due to the formation of these CO-Pd species. In addition, negative peaks around 3745–3784 cm^{-1} are observed in both Fig. 10a and b and can be related to acid hydroxyls of the zeolite structure that are interacting with NO [43–45].

Figure 11a and b compare the corresponding spectra for Pd-La/BEA during the adsorption at 80 °C, with and without CO for each cycle. The strongest peak in Fig. 11a is related to bidentate nitrate appearing at 1543 cm^{-1} [5], which can explain the greater thermal stability of adsorbed NO_x on the promoted sample. In Fig. 10a, this peak is much weaker for the unpromoted material. Examining the DRIFT spectra for La/BEA in dry and wet conditions (see Fig. S8) showed a clear peak at 1545 cm^{-1} related to bidentate nitrates [5]. It should be noted that for the in situ DRIFT equipment, there are some NO_2 present in the inlet feed, due to the low flow where NO and O_2 are pre-mixed in advance. Thus, the peak at 1543 cm^{-1} in the Pd-La/BEA is likely related to nitrates on or in close contact with the La.

The second strongest peak appeared at 1810 cm^{-1} for the Pd-La/BEA, which is assigned to Pd^{2+}-NO nitrosyls as mentioned earlier. The peak at 1813 cm^{-1} reduced with 5 and 11% for cycle 2 and 3 with high CO concentration compared to degreened catalyst (cycle 1) for Pd/BEA, while for Pd-La/BEA the numbers were 7 and 9% respectively. Thus, also DRIFTS results support the deactivation of the ion-exchanged Pd sites and that the Pd-La/BEA is more stable than Pd/BEA. However, it should be noted that DRIFTS is not a technique for quantification and should only be used for trends. The effect of CO on the NO storage is significantly less in DRIFTS compared to in flow reactor experiments and this is likely due to the different conditions regarding temperature in the ramp and gas composition. The weaker peak around 1307 cm^{-1} can be assigned to monodentate nitrates [46, 47]. Another peak appearing in the La containing sample was located at 1608 cm^{-1} which is related to bridging bidentate nitrates [10]. Similar to the Pd/BEA spectra, negative peaks are formed between 2000 and 2127 cm^{-1} (Fig. 11a) for cycles 2 and 3, which is a result of the removal of Pd-CO species during NO adsorption without the presence of CO. Correspondingly, these peaks appeared as positive peaks when CO was present in the feed gas (Fig. 11b). The desorption step reaching up to about 340 °C in the catalyst bed was likely not be sufficient for CO removal. Therefore, the remaining CO was released by NO replacement during the next step and caused the negative peak to appear.

From examination of the peaks around 3661–3784 cm^{-1} in the Pd/BEA and Pd-La/BEA samples, it can be seen that Pd/BEA has strong negative peaks in this area (Fig. 10). Many studies mentioned the formation of hydroxyl groups and water adsorption on Pd and it was shown that up to four water molecules can be coordinated to fully hydrated palladium ions [48, 49]. Paolucci et al. reported that OH groups can charge balance copper species in ion-exchanged Cu/SSZ-13 [50]. Accordingly, we suggest that OH groups can also charge balance Pd species at ion-exchanged sites in the zeolite and it is possible that there are adsorbed H_2O species on the Pd sites as well [5]. By adsorption of NO, these OH species can be displaced causing negative peaks to form [5], which is in line with the results in the current study. However, DRIFTS analysis of the La promoted sample shows that these negative peaks disappeared and thus it can be suggested that La either reduces the OH group formation or decreases the removal of them.

Comparison of Figs. 10 and 11 shows a clear difference, where the peak at 1543 cm^{-1} is significantly larger for the La containing sample, and nitrate peaks around 1307 cm^{-1} and 1608 cm^{-1} were also formed for Pd-La/BEA sample. Thus, the formation of nitrates was more significant in the promoted sample. The high thermal stability of nitrate bonds can explain the greater thermal stability of adsorbed NO_x on the promoted sample observed in the flow reactor TPD experiments (see Table 2). Thus, it can be concluded that the addition of La caused stronger NO_x bonds during adsorption and a relatively higher temperature is required for desorption of these species.

Regarding the stability of the adsorbents in the presence of high CO concentration, as shown in Figs. 10 and 11, the quantity of the adsorbed NO_x species gradually dropped due to the multiple cycles of TPD, which can be due to the formation of PdO_x clusters, as suggested by the oxygen TPD results.

4 Conclusions

In this study, it is concluded that La addition to Pd/BEA can promote the passive NO_x adsorber, to store more NO_x that is released in the medium temperature interval (200–400 °C). The Pd species are clearly affected by the presence of La, where the Pd oxidation state is lower for the Pd-La/BEA sample according to XPS measurements. In addition, Pd in Pd-La/BEA can adsorb oxygen with lower binding strength compared to Pd/BEA. We also found that La impregnation order on the Pd/BEA can play an important role in the PNA performance. Loading of Pd prior to La on the BEA support caused a greater quantity of NO_x to be released at temperatures higher than urea dosing. This was supported with TEM

analysis which showed a better distribution of particles in the Pd-La/BEA sample compared with La-Pd/BEA.

In addition, the performance stability of the adsorbent in multiple cold-start conditions in the presence of CO was studied with the Pd/BEA sample as a reference compared to the Pd-La/BEA sample. It was concluded that by increasing the number of cycles in the experiment, the Pd/BEA lost the weak bonded NO_x (desorbing below 200 °C) continuously throughout the 10 cycles. Moreover, 99% of the stronger bond NO_x, which was released between 200 and 400 °C, already vanished after the 5th cycle. In contrast, the promoted Pd-La/BEA sample retained 36% of the NO_x desorbed in the medium temperature range after the 5th cycle, and the NO_x release was not further decreased up to the 10th cycle. These results were supported by DRIFTS analysis, which indicated that the intensity of the formed NO_x species gradually decreased.

The O_2-TPD characterization results suggest that the deactivation was due to loss of active sites (Pd^{2+}) through the cycles by the formation of large amounts of PdO_x clusters on the surface. The results also clearly showed that there was less PdO_x formed for the La-doped sample during cycles with the presence of CO, which is in line with the NO TPD results. XPS results also showed a clear shift for Pd for the reacted Pd/BEA sample toward lower binding energies which is most likely due to reduction of ionic Pd to metallic Pd. Metallic Pd can thereafter form PdO_x clusters in the form of agglomerated particles [22]. For Pd-La/BEA on the other hand, a lower Pd oxidation state was found for the degreened sample, which increased after the aging, also suggesting more PdO_x formation. The O_2-TPD experiments showed an increased PdO_x formation for both samples during cycles with the presence of CO, but that the increase was significantly larger for the Pd/BEA sample.

In order to further elucidate the role of lanthanum, the NO adsorption stability experiments were also performed with a Pd-free sample (La/BEA). The results showed that also La/BEA can store NO_x, but that the Pd-La/BEA releases 61% more NO_x below 400 °C compared to La/BEA. DRIFTS showed that the storage on La/BEA was mainly originating from nitrates, and these species were also found for the Pd-La/BEA sample. The nitrates on La were stable during the CO cycling and therefore the La/BEA only lost a small amount of its storage capacity. The nitrates could be formed by small amounts of NO_2 in the feed and possibly by conversion of NO to nitrates over Pd (for Pd-La/BEA) since the samples exhibit NO oxidation capacity. The last cycle (10th cycle) showed that Pd-La/BEA still released more NO_x (18%) compared to La/BEA in the region 200–400 °C. In addition, there are large differences in the transient behavior for the storage and release for the two samples, suggesting that for the Pd-La/BEA sample after multiple cycles both the Pd and La storage are important. The NO_x release for the Pd-La/BEA sample occurred in a better temperature region (peak temperature at 289 °C), while La/BEA desorbed the NO_x at a high temperature (364 °C). The presence of Pd facilitated NO_x desorption. In addition, the Pd-La/BEA clearly adsorbed significant amounts of NO during the temperature ramp (49% of the total released NO_x), unlike the La/BEA sample, which likely adsorbed mostly small amounts of NO_2 present in the inlet feed.

Supplementary Information The online version contains supplementary material available at https://doi.org/10.1007/s40825-021-00205-2.

Acknowledgements This work was performed at Chemical Engineering and the Competence Centre for Catalysis, Chalmers University of Technology. We thank Stefan Gustavsson at CMAL at the Chalmers University of Technology for the help with the TEM measurements. We gratefully acknowledge the funding from the Swedish Research Council (642-2014-5733).

Funding Open access funding provided by Chalmers University of Technology.

Declarations

Ethics Approval On behalf of all the co-authors, the corresponding author states there is not any violations or inconsistencies to the ethics standards.

Consent to Participate On behalf of all the co-authors, the corresponding author confirms the consent to participate

Consent for Publication On behalf of all the co-authors, the corresponding author confirms the consent for the publication

Conflict of Interest The authors declare that they have no competing interests.

References

1. Beale, A.M., Gao, F., Lezcano-Gonzalez, I., Peden, C.H., Szanyi, J.: Recent advances in automotive catalysis for NOx emission control by small-pore microporous materials. Chem. Soc. Rev. **44**(20), 7371–7405 (2015). https://doi.org/10.1039/C5CS00108K
2. Forzatti, P., Nova, I., Tronconi, E.: New "Enhanced NH3-SCR" Reaction for NOx emission control. Ind. Eng. Chem. Res. **49**(21), 10386–10391 (2010). https://doi.org/10.1021/ie100600v

3. Xie, K., Woo, J., Bernin, D., Kumar, A., Kamasamudram, K., Olsson, L.: Insights into hydrothermal aging of phosphorus-poisoned Cu-SSZ-13 for NH3-SCR. Appl. Catal. B. **241**, 205–216 (2019). https://doi.org/10.1016/j.apcatb.2018.08.082
4. De Abreu Goes, J.E., Olsson, L., Berggrund, M., Kristoffersson, A., Gustafson, L., Hicks, M.: Performance studies and correlation between vehicle- and rapid- aged commercial lean NOx trap catalyst. SAE Int. J. Engines. **10**(4), 1613–1626 (2017). https://doi.org/10.4271/2017-01-0940
5. Mihai, O., Trandafilović, L., Wentworth, T., Torres, F.F.: Olsson, L,: The effect of Si/Al ratio for Pd/BEA and Pd/SSZ-13 used as passive NOx adsorbers. Top. Catal. **61**(18), 2007–2020 (2018). https://doi.org/10.3390/ma12071045
6. Jones, S., Ji, Y., Bueno-Lopez, A., Song, Y.: Crocker, M,: CeO2-M2O3 Passive NOxAdsorbers for cold start applications. Emiss. Control Sci. and Technol. **3**(1), 59–72 (2017). https://doi.org/10.1007/s40825-016-0058-7
7. Porta, A., Pellegrinelli, T., Castoldi, L., Matarrese, R., Morandi, S., Dzwigaj, S.: Lietti, L,: Low temperature NOx adsorption study on Pd-promoted zeolites. Top. Catal. **61**(61–19), 2021–2034 (2018). https://doi.org/10.1007/s11244-018-1045-8
8. Schmeisser, V., Weibel, M., Hernando, L.S., Nova, I., Tronconi, E., Ruggeri, M.P.: Cold start effect phenomena over zeolite SCR catalysts for exhaust gas aftertreatment. SAE Int. J. Commer. Veh. **6**(1), 190–199 (2013). https://doi.org/10.4271/2013-01-1064
9. Iwasaki, M., Shinjoh, H.: A comparative study of "standard", "fast" and "NO2" SCR reactions over Fe/zeolite catalyst. Appl. Catal. **390**, 71–77 (2010). https://doi.org/10.4271/2013-01-1064
10. Ji, Y., Bai, S., Crocker, M.: Al2O3-based passive NOx adsorbers for low temperature applications. Appl. Catal. B. **170**, 283–292 (2015). https://doi.org/10.1016/j.apcatb.2015.01.025
11. Ren, S., Schmieg, S.J., Koch, C.K., Qi, G., Li, W.: Investigation of Ag-based low temperature NOx adsorbers. Catal. **258**, 378–385 (2015). https://doi.org/10.1016/j.cattod.2015.02.008
12. Kyriakidou, E.A., Lee, J., Choi, J.S., Lance, M., Toops, T.J.: A comparative study of silver- and palladium-exchanged zeolites in propylene and nitrogen oxide adsorption and desorption for cold-start applications. Catal. Today **360**, 220–233 (2021)
13. Ji, Y., Xu, D., Bai, S., Graham, U., Crocker, M., Chen, B., Graham, U., Shi, C., Harris, D., Scapens, D., Darab, J.: Pt- and Pd-promoted CeO2–ZrO2 for passive NOx adsorber applications. Ind. Eng. Chem. Res. **56**(1), 111–125 (2017). https://doi.org/10.1021/acs.iecr.6b03793
14. Tamm, S., Andonova, S., Olsson, L.: Silver as storage compound for NOx at low temperatures. Catal. Lett. **144**(4), 674–684 (2014). https://doi.org/10.1007/s10562-014-1211-y
15. Chen, H.-Y., Collier, J.E., Liu, D., Mantarosie, L., Durán-Martín, D., Novák, V., et al.: Low temperature NO storage of zeolite supported Pd for low temperature diesel engine emission control. Catal. Lett. **146**(9), 1706–1711 (2016). https://doi.org/10.1007/s10562-016-1794-6
16. Ryou, Y., Lee, J., Lee, H., Kim, C.H., Kim, D.H.: Effect of sulfur aging and regeneration on low temperature NO adsorption over hydrothermally treated Pd/CeO2 and Pd/Ce0. 58Zr0. 42O2 catalysts. Catal. **297**, 53–59 (2017). https://doi.org/10.1016/j.cattod.2017.06.035
17. Zheng, Y., Kovarik, L., Engelhard, M.H., Wang, Y., Wang, Y., Gao, F., Szanyi, J.: Low-temperature Pd/zeolite passive NOx adsorbers: structure, performance, and adsorption chemistry. J. Phys. Chem. C. **121**(29), 15793–15803 (2017). https://doi.org/10.1021/acs.jpcc.7b04312
18. Ilmasani, R.F., Woo, J., Creaser, D., Olsson, L.: Influencing the NOx stability by metal oxide addition to Pd/BEA for passive NOx adsorbers. Ind. Eng. Chem. Res. **59**(21), 9830–9840 (2020). https://doi.org/10.1021/acs.iecr.9b06976
19. Vu, A., Luo, J., Li, J., Epling, W.S.: Effects of CO on Pd/BEA passive NOx adsorbers. Catal. Lett. **147**(3), 745–750 (2017). https://doi.org/10.1007/s10562-017-1976-x
20. YuntaoGu, R.P.Z., Chen, Yu-Ren., William Epling, S.: Investigation of an irreversible NOx storage degradation mode on a Pd/BEA passive NOx adsorber. Appl. Catal. B. **258**, 118032 (2019). https://doi.org/10.1016/j.apcatb.2019.118032
21. Theis, J.R., Ura, J.A.: Assessment of zeolite-based low temperature NOx adsorbers: effect of reductants during multiple sequential cold starts. Catal. (2020). https://doi.org/10.1016/j.cattod.2020.01.040
22. Lardinois, T.M., Bates, J.S., Lippie, H.H., Russell, C.K., Miller, J.T., Meyer, H.M., Unocic, K.A., Prikhodko, V., Wei, X., Lambert, C.K., Getsoian, A.B., Gounder, R.: Structural interconversion between agglomerated palladium domains and mononuclear Pd(II) Cations in Chabazite Zeolites. Chem. Mater. **33**, 1698–1713 (2021)
23. Ryou, Y., Lee, J., Cho, S.J., Lee, H., Kim, C.H., Kim, D.H.Y.: Activation of Pd/SSZ-13 catalyst by hydrothermal aging treatment in passive NO adsorption performance at low temperature for cold start application. Appl. Catal. B. **212**, 140–149 (2017). https://doi.org/10.1016/j.apcatb.2017.04.077
24. Yasumura, S., Ide, H., Ueda, T., Jing, Y., Liu, C., Kon, K., Toyao, T., Maeno, Z., Shimizu, K.-I.: Transformation of bulk Pd to Pd cations in small-pore CHA zeolites facilitated by NO. JACS. **1**, 201–211 (2021)
25. Hoost, T., Otto, K.: Temperature-programmed study of the oxidation of palladium/alumina catalysts and their lanthanum modification. Appl. Catal. A-Gen. **92**(1), 39–58 (1992). https://doi.org/10.1016/0926-860X(92)80278-K
26. Friberg, I., Sadokhina, N., Olsson, L.: The effect of Si/Al ratio of zeolite supported Pd for complete CH4 oxidation in the presence of water vapor and SO2. Appl. Catal. B. **250**, 117–131 (2019). https://doi.org/10.1016/j.apcatb.2019.03.005
27. Yu, Y., Takei, T., Ohashi, H., He, H., Zhang, X., Haruta, M.: Pretreatments of Co3O4 at moderate temperature for CO oxidation at −80°C. J. Catal. **267**(2), 121–128 (2009). https://doi.org/10.1016/j.jcat.2009.08.003
28. Lou, Y., Ma, J., Hu, W., Dai, Q., Wang, L., Zhan, W., Guo, Y., Cao, X.-M., Guo, Y., Hu, P., Lu, G.: Low-temperature methane combustion over Pd/H-ZSM-5: active Pd sites with specific electronic properties modulated by acidic sites of H-ZSM-5. ACS Catal. **6**(12), 8127–8139 (2016). https://doi.org/10.1021/acscatal.6b01801
29. Simplício, L.M.T., Brandão, S.T., Sales, E.A., Lietti, L., Bozon-Verduraz, F.: Methane combustion over PdO-alumina catalysts: The effect of palladium precursors. Appl. Catal. B. **63**(1), 9–14 (2006). https://doi.org/10.1016/j.apcatb.2005.08.009
30. Weast, R.C., Astle, M.J., Beyer, W.H.: CRC handbook of chemistry and physics, 64th edn. CRC Press, Boca Raton, FL (1988)
31. Buzková Arvajová, A., Boutikos, P., Pečinka, R., Kočí, P.A.: Global kinetic model of NO oxidation on Pd/γ-Al2O3 catalyst including PdOx formation and reduction by CO and C3H6. Appl. Catal. B. **260**, 118141 (2020). https://doi.org/10.1016/j.apcatb.2019.118141
32. Ryou, Y., Lee, J., Kim, Y., Hwang, S., Lee, H., Kim, C.H., Kim, D.H.: Effect of reduction treatments (H2 vs. CO) on the NO adsorption ability and the physicochemical properties of Pd/SSZ-13 passive NOx adsorber for cold start application. Appl. Catal. A-Gen. **569**, 28–34 (2019). https://doi.org/10.1016/j.apcata.2018.10.016
33. Guascito, M.R., Cesari, D., Chirizzi, D., Genga, A., Contini, D.: XPS surface chemical characterization of atmospheric particles of different sizes. Atoms. **116**, 146–154 (2015)
34. Datye, A.K., Bravo, J., Nelson, T.R., Atanasova, P., Lyubovsky, M., Pfefferle, L.: Catalyst microstructure and methane oxidation

reactivity during the Pd↔PdO transformation on alumina supports. Appl. Catal. A-Gen. **198**(1), 179–196 (2000). https://doi.org/10.1016/S0926-860X(99)00512-8
35. Arunagiri, T., Golden, T.D., Chyan, O.: Study of palladium metal particle deposition on the conductive diamond surface by XRD, XPS and electrochemistry. Mater. Chem. Phys. **92**, 152–158 (2005). https://doi.org/10.1016/j.matchemphys.2005.01.005
36. Kim, D.H., Woo, S.I., Lee, J.M., Yang, O.B.: The role of lanthanum oxide on Pd-only three-way catalysts prepared by co-impregnation and sequential impregnation methods. Catal. Lett. **70**, 35–41 (2000). https://doi.org/10.1023/A:1019083704188
37. Crocoll, M., Kureti, S., Weisweiler, W.: Mean field modeling of NO oxidation over Pt/Al2O3 catalyst under oxygen-rich conditions. J. Catal. **229**(2), 480–489 (2005). https://doi.org/10.1016/j.jcat.2004.11.029
38. Shwan, S., Nedyalkova, R., Jansson, J., Korsgren, J., Olsson, L., Skoglundh, M.: Influence of hydrothermal ageing on NH3-SCR over Fe-BEA—inhibition of NH3-SCR by ammonia. Top Catal. **59**, 80–88 (2013). https://doi.org/10.1007/s11244-013-9933-4
39. Kim, Y., Hwang, S., Lee, J., Ryou, Y., Lee, H., Kim, C.H., Kim, D.H.Y.: Comparison of NOx adsorption/desorption behaviors over Pd/CeO2 and Pd/SSZ-13 as passive NOx adsorbers for cold start application. Emission Contr. Sci. Technol. **5**(2), 172–182 (2019). https://doi.org/10.1007/s40825-019-00119-0
40. Wang, A., Xie, K., Kumar, A., Kamasamudram, K., Olsson, L.: Layered Pd/SSZ-13 with Cu/SSZ-13 as PNA − SCR dual-layer monolith catalyst for NOx abatement. Catal. (2020)https://doi.org/10.1016/j.cattod.2020.01.035
41. Khivantsev, K., Jaegers, N.R., Kovarik, L., Hanson, J.C., Tao, F., Tang, Y., Zhang, X., Koleva, I.Z., Aleksandrov, H.A., Vayssilov, G.N., Wang, Y., Gao, F., Szanyi, J.: Achieving atomic dispersion of highly loaded transition metals in small-pore zeolite SSZ-13: high-capacity and high-efficiency low-temperature CO and passive NOx adsorbers. Angew. Chem. Int. Ed. **57**(51), 16672–16677 (2018). https://doi.org/10.1002/anie.201809343
42. Zhu, H., Qin, Z., Shan, W., Shen, W., Wang, J.: Pd/CeO2–TiO2 catalyst for CO oxidation at low temperature: a TPR study with H2 and CO as reducing agents. J. Catal. **225**(2), 267–277 (2004). https://doi.org/10.1016/j.jcat.2004.04.006
43. Descorme, C., Gélin, P., Primet, M., Lécuyer, C.: Infrared study of nitrogen monoxide adsorption on palladium ion-exchanged ZSM-5 catalysts. Catal. Lett. **41**(3), 133–138 (1996). https://doi.org/10.1007/BF00811479
44. Gupta, A., Kang, S. B., Harold, M. P.: NOx uptake and release on Pd/SSZ-13: Impact of feed composition and temperature. Catal. (2020)https://doi.org/10.1016/j.cattod.2020.01.018
45. Ambast, M., Karinshak, K., Rahman, B. M. M., Grabow, L. C., Harold, M. P.: Passive NOx adsorption on Pd/H-ZSM-5: experiments and modeling, Appl. Catal. B. 118802 (2020) https://doi.org/10.1016/j.apcatb.2020.118802
46. Meunier, F., Zuzaniuk, V., Breen, J., Olsson, M., Ross, J.: Mechanistic differences in the selective reduction of NO by propene over cobalt-and silver-promoted alumina catalysts: kinetic and in situ DRIFTS study. Catal. **59**(3–4), 287–304 (2000). https://doi.org/10.1016/S0920-5861(00)00295-9
47. Westerberg, B., Fridell, E.: A transient FTIR study of species formed during NOx storage in the Pt/BaO/Al2O3 system. J. Mol. Catal. A Chem. **165**, 249–263 (2001). https://doi.org/10.1016/S1381-1169(00)00431-3
48. Sadokhina, N., Ghasempour, F., Auvray, X., Smedler, G., Nylén, U., Olofsson, M., Olsson, L.: An experimental and kinetic modelling study for methane oxidation over Pd-based catalyst: inhibition by water. Catal. Lett. **147**, 2360–2371 (2017). https://doi.org/10.1007/s10562-017-2133-2
49. Aakesson, R., Pettersson, L.G.M., Sandstroem, M., Wahlgren, U.: Ligand field effects in the hydrated divalent and trivalent metal ions of the first and second transition periods. J. Am. Chem. Soc. **116**(19), 8691–8704 (1994). https://doi.org/10.1021/ja00098a032
50. Paolucci, C., Parekh, A.A., Khurana, I., Di Iorio, J.R., Li, H., Albarracin Caballero, J.D., Shih, A.J., Anggara, T., Delgass, W.N., Miller, J.T., Ribeiro, F.H., Gounder, R., Schneider, W.F.: Catalysis in a cage: condition-dependent speciation and dynamics of exchanged Cu cations in SSZ-13 zeolites. J. Am. Chem. Soc. **138**(18), 6028–6048 (2016). https://doi.org/10.1021/jacs.6b02651